

The Effect of Pre-Reduction of Graphene Oxide on the Electrochemical Performance of rGO-TiO₂ Nanocomposite

Z. Abasali karaj abad¹, A. Nemati^{1*}, A. Malek Khachatourian¹ and M. Golmohammad²

*nemati@sharif.edu

Received: April 2020

Revised: June 2020

Accepted: July 2020

¹ Department of Materials Science and Engineering, Sharif University of Technology, Tehran, Iran

² Renewable Energy Department, Niroo Research Institute (NRI), Tehran, Iran

DOI: 10.22068/ijmse.17.4.55

Abstract: The graphene oxide -TiO₂ (GO-TiO₂) and pre-reduced graphene oxide -TiO₂ (rGO-TiO₂) nanocomposites were fabricated successfully by hydrothermal method. The microstructure of synthesized nanocomposites was investigated using field emission scanning electron microscopy (FESEM) equipped with energy dispersive spectroscopy (EDS) analysis. Moreover, galvanostatic charge/discharge (GCD), cyclic voltammetry (CV), and electrochemical impedance spectroscopy (EIS) methods in three electrode system were applied to evaluate electrochemical properties. The FESEM results clearly showed the formation of TiO₂ nanoparticles with average particle size of 25 nm on graphene sheets in both samples. The rGO-TiO₂ and GO-TiO₂ nanocomposites showed 224 and 32 F/g specific capacitance at 5 mV s⁻¹ scan rate in 1 M KOH aqueous electrolyte, respectively. The pre-reduction of graphene oxide is the main reason for the better electrochemical performance of rGO-TiO₂ compared to GO-TiO₂ nanocomposite samples.

Keywords: Pre-reduction, Nanocomposite, Hydrothermal, Reduced Graphene Oxide, Supercapacitor, TiO₂.

1. INTRODUCTION

The ever-expanding need for portable electronic devices such as laptops, mobiles, and electric vehicles, as well as the non-renewability of fossil fuel sources and their environmental pollution, are major reasons that have led to extensive research on renewable energy sources and consequently the development of energy storage devices [1-3]. Electrochemical capacitors (ECs), also known as supercapacitors (SCs), are believed to be one of the most promising and practical energy storage devices, due to their fast charge-discharge rates, high power density (compared with batteries), simple mechanism, and long life cycle [4]. Carbon materials, conducting polymers, and transition metal oxides are three families of the electrode materials for SCs [5, 6]. It is well known that the electrode materials mainly rule the performances of SCs.

The energy storage mechanism of transition metal oxides such as MnO₂, RuO₂, ZnO, and TiO₂ are based on the reversible and very fast redox reactions which result in higher charge storage and specific capacity of SCs [5, 7]. Unfortunately, during the redox processes, the structures of these metal oxides can be easily damaged which can result in low electrical conductivity and poor cycling stabilities and restrict the use of these materials as electrodes in the SCs [8, 9].

It seems that the hybridization of transition metal oxides with carbon materials, especially graphene with exceptional thermal, mechanical, and electrical properties, can improve the efficiency of electrode materials by increasing the specific capacity of SCs [10, 11]. Today, the chemical exfoliation method is commonly used to synthesize graphene. In this method, graphite should be converted first to graphene oxide (GO) using strong oxidizing agents, a nonconductive hydrophilic carbon material, afterward, by removing oxygen functional groups, reduced graphene oxide (rGO) can be obtained [11]. Therefore recently graphene based nanocomposites such as rGO-ZnO, rGO-Fe₂O₃, rGO-RuO₂, rGO-MnO₂, and rGO-TiO₂ have been considered as efficient electrode materials in supercapacitors [10, 12 and 13].

Among these materials, rGO-TiO₂ nanocomposite has attracted the attention of many researchers due to low cost, nontoxicity, eco-friendliness, the high specific energy density, and abundant availability of TiO₂ [14, 15]. For example, Mishra et al. decorated TiO₂ nanoparticles over functionalized graphene by sol-gel method [16]. Xiang et al. used the hydrothermal method to synthesized rGO/TiO₂ nanobelts and nanoparticles as SC electrodes. Their results revealed a specific capacitance of 200 and 60Fg⁻¹ at a scan rate of 2mVs⁻¹, but only

56.2 and 18.4F/g at a scan rate of 100mVs^{-1} , for nanobelts and nanoparticles, respectively [17]. Sun et al. used atomic layer deposition to coat graphene sheets with TiO_2 nanoparticles and demonstrated a specific capacitance of 75Fg^{-1} at a scan rate of 10mVs^{-1} [18]. Liu et al. have also investigated a GO/TiO_2 nanorod composite to attain a specific capacitance of 100F/g at 5mVs^{-1} scan rate [19].

Reduction of GO make changes in its physical and chemical properties [20], so it appears that the pre-reduction of GO will also affect the electrochemical properties of GO/TiO_2 nanocomposite. The latter point has not been studied by other researchers to the best of authors' knowledge.

In this research, the effect of pre-reduction of graphene oxide before the composite formation process on the quality of the synthesized nanocomposite and its electrochemical performance were examined. For this purpose, $\text{GO}-\text{TiO}_2$ and $\text{rGO}-\text{TiO}_2$ nanocomposites were synthesized using the hydrothermal process. Reduced graphene oxide, which was reduced for 18 hours, was used as a precursor for $\text{rGO}-\text{TiO}_2$ nanocomposite sample synthesis.

2. EXPERIMENTAL PROCEDURE

All chemical reagents with analytical grade used as received in this work (Merck, analytical grade). (For Hummers method: Graphite powder as precursor of GO, potassium permanganate (KMnO_4), phosphoric (H_3PO_4), sulfuric acid (H_2SO_4 98%) and hydrogen peroxide as strong oxidizers, ethanol, acetone, deionized (DI) water and hydrochloric acid (HCl) for washing), titanium tetraisopropoxide (TTIP) as precursor of TiO_2 , Potassium hydroxide (KOH) as electrolyte and nickel foam.

The graphene oxide (GO) was fabricated using an improved Hummers method [11]. For the synthesis of nanocomposite samples, first 0.4 ml of TTIP was added drop-wise to 10 ml of ethanol under vigorous stirring for 1 hour (IKA Magnetic Stirrers, RCT basic). 8 ml of the resulting solution was added dropwise to the 20 mL of GO suspension (2mg mL^{-1}) and stirred for 1 hour and was placed in an ultrasonic bath (GRANT_17002) for one hour (volumetric ratio of TTIP: GO suspension was 0.016). Afterwards, it was poured into a 40 ml autoclave and heated at

$180\text{ }^\circ\text{C}$ for 12 hours. Finally, the autoclave was allowed to reach room temperature and its contents were washed three times with DI water. It was then dried at $70\text{ }^\circ\text{C}$ in an oven to obtain $\text{GO}-\text{TiO}_2$ powder. The same steps were taken to synthesize $\text{rGO}-\text{TiO}_2$ nanocomposite samples, except that the reduced graphene oxide suspension, which was reduced for 18 hours via hydrothermal process at $180\text{ }^\circ\text{C}$, was used instead of the graphene oxide suspension. The microstructural study of the $\text{GO}-\text{TiO}_2$ and $\text{rGO}-\text{TiO}_2$ nanocomposites were conducted using field emission scanning electron microscope (FESEM) equipped with energy dispersive spectroscopy (EDS) analysis (MIRA3 TESCAN-XMU).

Cyclic voltammetry (CV) in a potential window from 0 V to 0.5 V for $\text{GO}-\text{TiO}_2$, and 0 V to 0.65 V for $\text{rGO}-\text{TiO}_2$ at 5, 10, 30, 50 and 100 mV/s scan rates, galvanostatic charge/discharge (GCD) at current density 1 A g^{-1} in the same potential window, and electrochemical impedance spectroscopy (EIS) at frequency range of 0.1 Hz-100 KHz, with 10 mV AC amplitude, of the $\text{GO}-\text{TiO}_2$ and $\text{rGO}-\text{TiO}_2$ nanocomposites were all evaluated using Auto-lb (PGSTAT 302N) and three-electrode system including a counter electrode (Pt wire), reference electrode (Ag/AgCl), and a working electrode (Ni foam-coated $\text{GO}-\text{TiO}_2$ and $\text{rGO}-\text{TiO}_2$ nanocomposites) all three electrodes were immersed in 1 M KOH aqueous solution.

3. RESULTS AND DISCUSSION

The FESEM images of $\text{GO}-\text{TiO}_2$ and $\text{rGO}-\text{TiO}_2$ nanocomposite samples at different magnifications are shown in Fig. 1. The microstructures clearly reveal the formation of nanoparticles with average particle size of 25 nm on graphene sheets in both samples. However, as can be seen, non-uniformity and concentration of nanoparticles at the surface of the sheets in $\text{GO}-\text{TiO}_2$ nanocomposite is higher than those in $\text{rGO}-\text{TiO}_2$ nanocomposite. It should be noted that the density of TiO_2 nanoparticles on graphene sheets in $\text{GO}-\text{TiO}_2$ nanocomposite is so high that graphene sheets are covered with agglomerated nanoparticles. It seems that the removal of the oxygen functional groups (which act as suitable sites for binding nanoparticles to the graphene sheets) from graphene sheets during the pre-reduction process has led to a decrease in the

concentration of nanoparticles in the rGO-TiO₂ nanocomposite.

Elemental map analysis of GO-TiO₂ and rGO-TiO₂ nanocomposites is shown in Figs. 2a, and Fig. 2b, respectively. These images also reveal the presence of more TiO₂ particles on the

surface of graphene sheets in nanocomposite GO-TiO₂ than in rGO-TiO₂ nanocomposite. According to Fig. 2 due to the pre-reduction process in rGO-TiO₂ nanocomposite synthesis, the density of oxygen atoms is lower than in GO-TiO₂ nanocomposite sample.

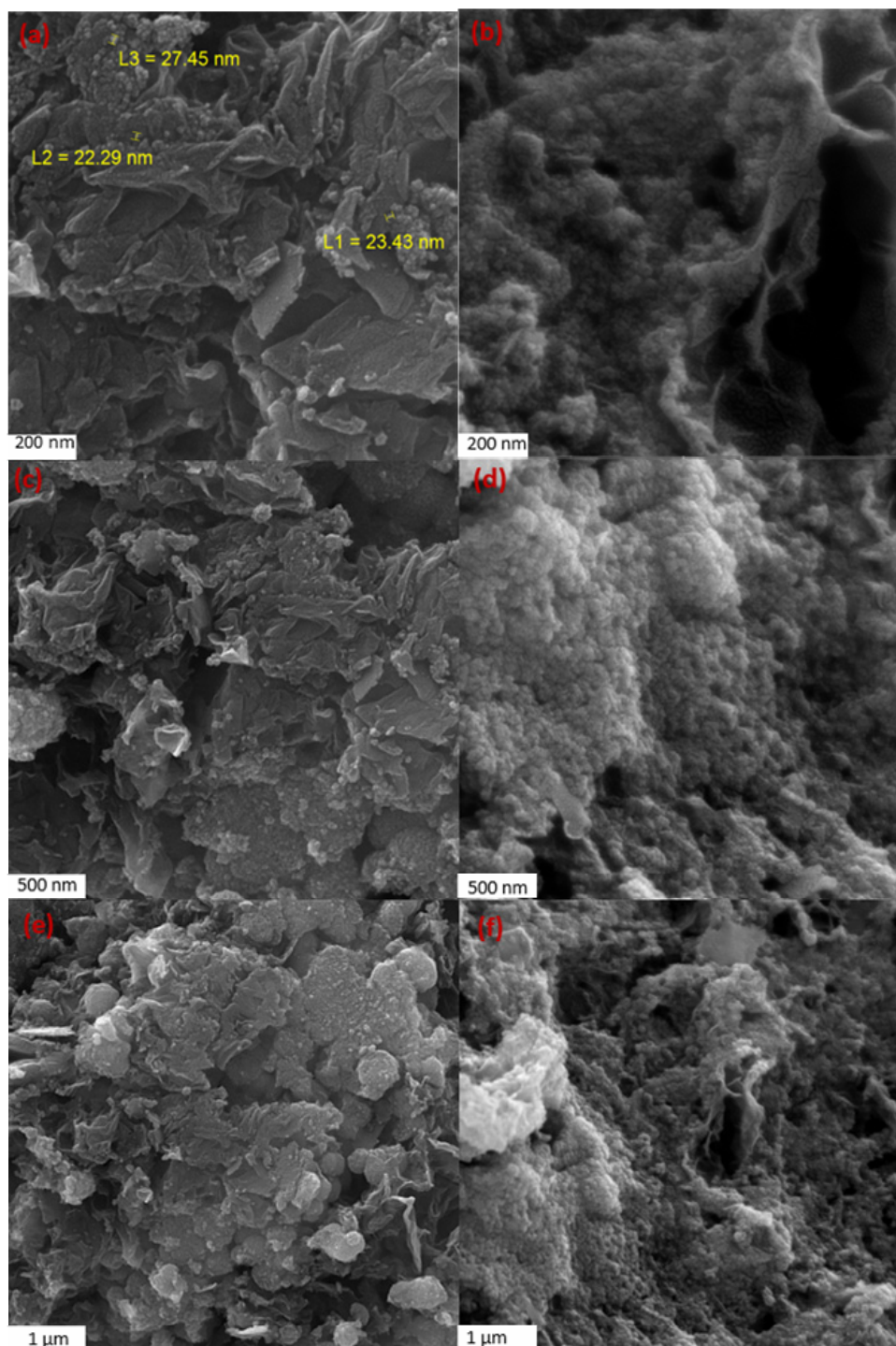


Fig. 1. FESEM images of rGO-TiO₂ (a, c, and e) and GO-TiO₂ (b, d, and f) nanocomposites at different magnifications.

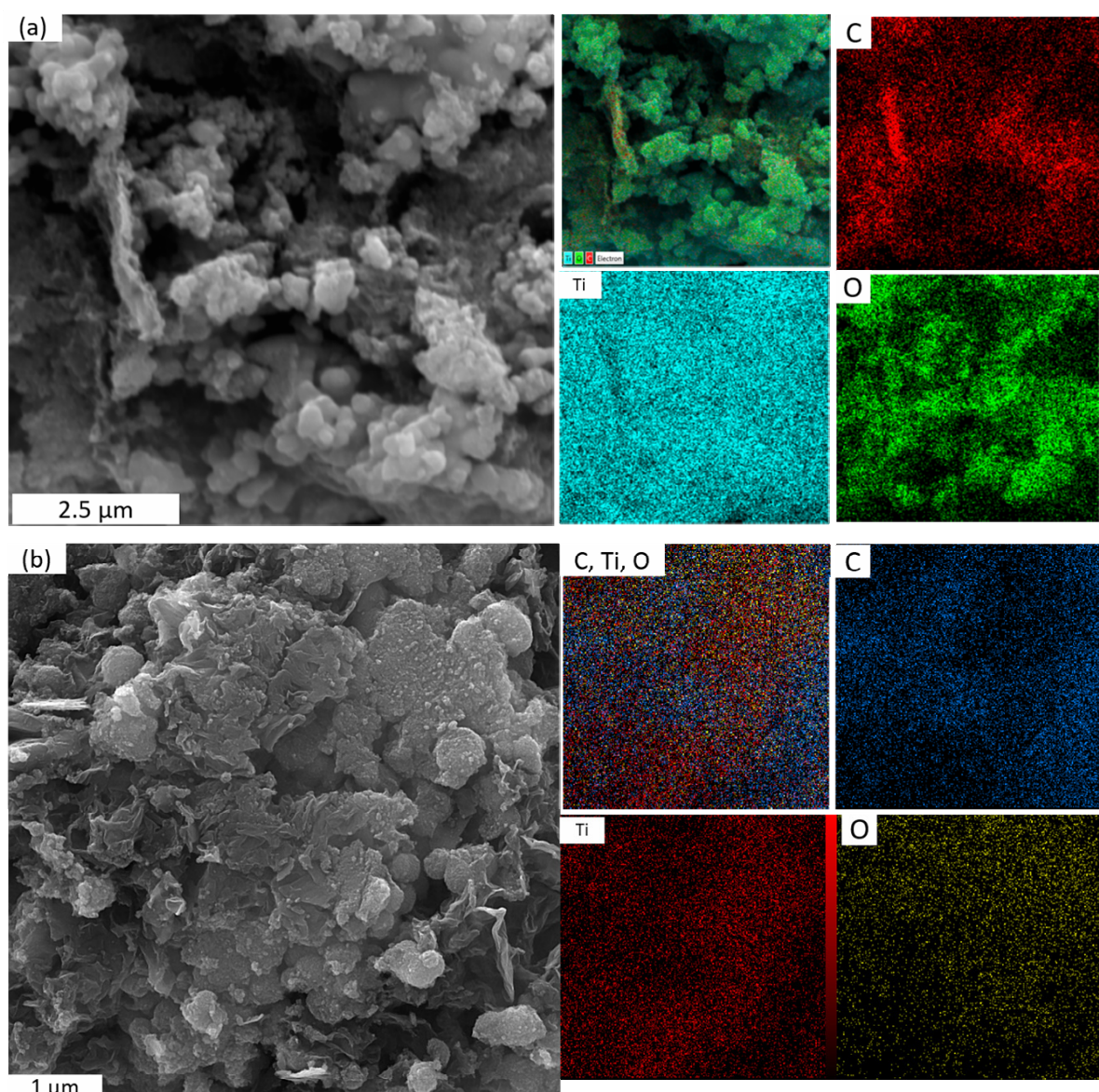


Fig. 2. Elemental map analysis of GO-TiO₂ (a) and rGO-TiO₂ (b) nanocomposite samples.

In order to evaluate the electrochemical performance of nanocomposites, CV test was performed in a potential window from 0 V to 0.5 V for GO-TiO₂, and 0 V to 0.65 V for rGO-TiO₂ at different scan rates (Fig. 3a and Fig. 3b respectively). A pair of redox peaks can be observed in the CV curves of rGO-TiO₂ nanocomposite (Fig. 3b), which indicates the existence of a pseudocapacitance mechanism in the charge storage [21]. Additionally, the double layer mechanism also might play a minor role in charge storage in this nanocomposite. While in the CV curves of GO-TiO₂ nanocomposite (Fig. 3a) no specific peak was observed and the charge storage mechanism was mainly due to the

electrical double layer. For comparison, in Fig. 3c, the CV curves of both nanocomposites are re-drawn at a scan rate of 50 mV s⁻¹ in the same plot. The much wider CV curve of the rGO-TiO₂ nanocomposite shows the better electrochemical performance of this nanocomposite. The specific capacitance of each electrode was calculated using the following equation (Eq. 1):

$$C = \frac{1}{2m\nu\Delta V} \int i dV \quad (1)$$

Where, *m* is the mass (g) of the electrode, *ν* is the scan rate (V/s), ΔV is the potential window (V), *i* is the current (A), and $\int i dV$ is the integration area for the CV curves [22]. The specific capacitance values of rGO-TiO₂ and

GO-TiO₂ nanocomposites were obtained 224 and 32 F/g at 5 mV s⁻¹ scan rate, respectively. The results indicated that the pre-reduction of graphene oxide has led to a multiplier increase in the specific capacity.

The GCD curves of rGO-TiO₂ and GO-TiO₂ nanocomposites at a current density of 1 A g⁻¹ is shown in Fig. 4. The shape of the GCD curve of nanocomposites is quite different. The shape of the GCD curve of GO-TiO₂ nanocomposite is similar to an isosceles triangle, while the shape of the GCD curve of rGO-TiO₂ nanocomposite is out of symmetrical shape and has areas with constant potential which indicates the presence of pseudo-capacitance behavior in this electrode [23]. It is also observed that the charge-discharge time of GO-TiO₂ nanocomposite (about 4 s) is much shorter than the charge-discharge time of rGO-TiO₂ nanocomposite (about 47 s). Generally, these curves confirm the superiority of rGO-TiO₂ nanocomposite electrochemical performance over rGO-TiO₂ nanocomposite,

which is in good agreement with CV results.

EIS test was performed (0.1 Hz - 100 KHz, with 10 mV AC amplitude) for rGO-TiO₂ and GO-TiO₂ nanocomposites, and the results are presented in the form of Nyquist plots in Fig. 5. It can be seen that internal resistance (R_s; determined by the intersection of plot on the left of the real axis) of rGO-TiO₂ nanocomposite (1.2Ω) is less than that of the GO-TiO₂ nanocomposite (2.5Ω)[24]. Therefore, it can be concluded that the pre-reduction of graphene oxide has led to a decrease in the internal resistance of the rGO-TiO₂ nanocomposite. Moreover, the higher slope of the linear part of the rGO-TiO₂ nanocomposite in the low frequency region indicates the rapid diffusion of ions and the high rate of double layer formation. According to the microstructure observed in FESEM images, it was predictable that the electrode material of the rGO-TiO₂ sample would have more access to electrolyte and faster ion diffusion.

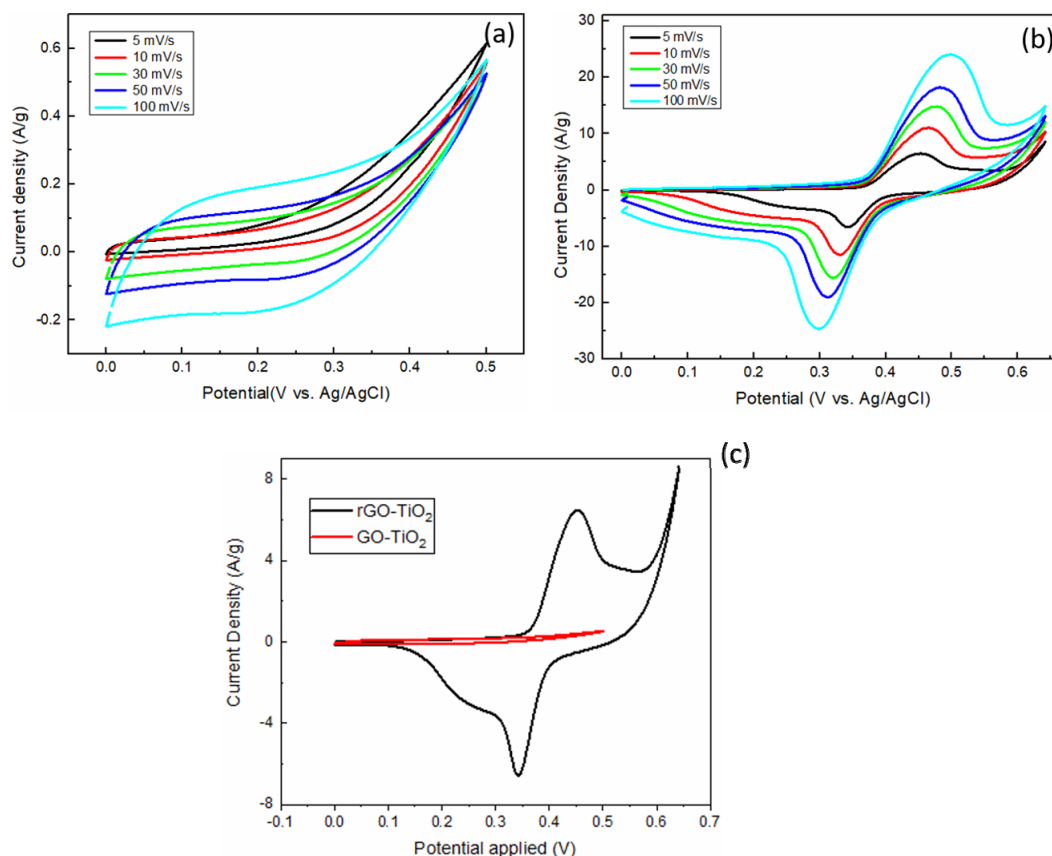


Fig. 3. CV curves of the GO-TiO₂ (a) and rGO-TiO₂ (b) nanocomposites at 5, 10, 30, 50 and 100 mV s⁻¹ scan rate, and GO-TiO₂ and rGO-TiO₂ nanocomposites at 50 mV s⁻¹ scan rate (c).

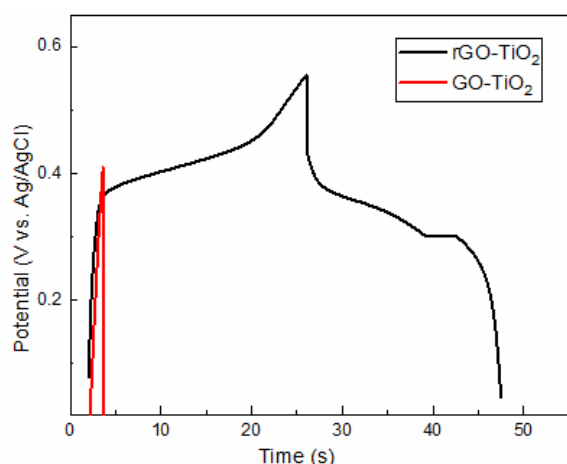


Fig. 4. GCD curve of rGO-TiO₂ and GO-TiO₂ nanocomposites at current density 1 A g⁻¹.

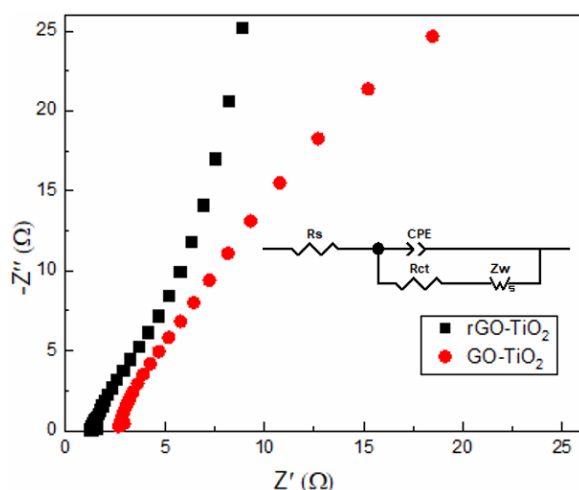


Fig. 5. Nyquist plots of EIS of rGO-TiO₂ and GO-TiO₂ nanocomposite samples

4. CONCLUSION

In this study, the effect of the pre-reduction of graphene oxide on the electrochemical performance of rGO-TiO₂ nanocomposite was investigated. FESEM images showed that using the pre-reduction process a more uniform and controlled distribution of nanoparticles on graphene sheets could be achieved. It was demonstrated that the nanocomposite samples made of pre reduced GO has better energy storage performance. The specific capacitance values of rGO-TiO₂ and GO-TiO₂ nanocomposites were 224 and 32 F/g at 5 mV s⁻¹ scan rate from CV curves, respectively. This significant increase in specific capacitance could be due to a decrease in the concentration of TiO₂ on graphene sheets, as both electrode materials,

graphene, and TiO₂, play an effective role in the energy storage process. Moreover, improvement in the electrochemical performance of rGO-TiO₂ nanocomposite electrodes was also observed by a longer charge-discharge process for this sample according to GCD results and lower internal resistance according to EIS results. Based on the results obtained in this study, the pre-reduction of graphene oxide can be used as an effective solution to increase the electrochemical efficiency of GO-TiO₂ nanocomposite samples.

5. REFERENCES

1. Yang, Zh., Zhang, j., Kintner-Meyer, M. C. W., Lu, X., Choi, D. and Lemmon, J. P., "Electrochemical energy storage for green grid," *J.Chem. Rev.*, 2011, 111, 3577–3613.
2. Singh, T. P. and Kumar, S. Y., "Comparative performance investigation of battery and ultracapacitor for electric vehicle applications," *Int. J. Appl. Eng. Res.*, 2017, 12, pp. 10197–10204.
3. Stoller, M. D., Park, S., Yanwu, Z., An, J. and Ruoff, R. S., "Graphene-Based ultracapacitors," *Nano Lett.*, 2008, 8, 3498–3502.
4. Wang, F., Xiao, S., Hou, Y., Hu, C., Liu, L. and Wu, Y., "Electrode materials for aqueous asymmetric supercapacitors," *RSC Adv.*, 2013, 3, 13059–13084.
5. Zheng, S., Wu, Z. S., Wang, S., Xiao, H., Zhou, F., Sun, Ch., Bao, X. and Cheng, H.M., "Graphene-based materials for high-voltage and high-energy asymmetric supercapacitors," *Energy Storage Mater.*, 2017, 6, 70–97.
6. Zeng, Y., Yu, M., Meng, Y., Fang, P., Lu, X. and Tong, Y., "Iron-Based Supercapacitor Electrodes: Advances and Challenges," *Adv. Energy Mater.*, 2016, 6, 1–17.
7. Augustyn, V., Simon, P. and Dunn, B., "Pseudocapacitive oxide materials for high-rate electrochemical energy storage," *Energy Environ. Sci.*, 2014, 7, 1597–1614.
8. Rajkumar, M., Hsu, C. T., Wu, T. H., Chen, M. G. and Hu, C. C., "Advanced materials for aqueous supercapacitors in the asymmetric design," *Prog. Nat. Sci. Mater. Int.*, 2015, 25, 527–544.
9. Aval, L. F., Ghoranneviss, M. and Pour, G. B., "High-performance supercapacitors

- based on the carbon nanotubes , graphene and graphite nanoparticles electrodes,” *Heliyon*, 2018 , 4, e00862.
10. Xu, X., Lin, Y., Huang, Z., Liu, X., Huang, Y. and Duan, Y., “Flexible Solid-State Supercapacitors Based on Three-Dimensional Graphene Hydrogel Films,” *ACS Nano*, 2013, 7, 4042–4049.
 11. Chen, J., Yao, B., Li, C. and Shi, G., “An improved Hummers method for eco-friendly synthesis of graphene oxide,” *Carbon N. Y.*, 2013, 64, 225–229.
 12. Wang, Y., Shi, Zh., Huang, Y., Ma, Y., Wang, Ch., Chen, M. and Chen., Y., “Supercapacitor Devices Based on Graphene Materials,” 2009, 113, 13103–13107.
 13. Stankovich, S., Dikin, D. A., Dommett, H. B., Kohlhaas, K. M., Zimney, E. J., Stach, E. A., Piner, R. D., Nguyen S. T. and Ruoff R. S., “Graphene-based composite materials,” *Nature*, 2006, 442, 282–286.
 14. Gobal F. and Faraji, M., “Electrochemical synthesis of reduced graphene oxide/TiO₂ nanotubes/Ti for high-performance supercapacitors,” *Ionics (Kiel)*, 2015, 21, 525–531.
 15. Sheha, E., “Studies on TiO₂/Reduced Graphene Oxide Composites as Cathode Materials for Magnesium-Ion Battery,” *Graphene*, 2014, 03, 36–43.
 16. Sundriyal, S., Sharma, M., Kaur, A., Mishra, S. and Deep, A., “Improved electrochemical performance of rGO/TiO₂ nanosheet composite based electrode for supercapacitor applications,” *J. Mater. Sci. Mater. Electron.*, 2018, 29, 12754–12764.
 17. Ates, M., Bayrak, Y., Yoruk, O. and Caliskan, S., “Reduced graphene oxide/Titanium oxide nanocomposite synthesis via microwave-assisted method and supercapacitor behaviors,” *J. Alloys Compd.*, 2017, 728, 541–551.
 18. Toledo, W. D., Couto, A. B., Almeida, D. A. L. and Ferreira, N. G., “Facile synthesis of TiO₂ /rGO neatly electrodeposited on carbon fiber applied as ternary electrode for supercapacitor,” *Mater. Res. Express*, 2019, 6, 065040.
 19. Ding, Y., Bai, W., Sun, J., Wu, Y., Memon, M. A., Wang, Ch., Liu, Ch., Huang, Y. and Geng J., “Cellulose Tailored Anatase TiO₂ Nanospindles in Three-Dimensional Graphene Composites for High-Performance Supercapacitors,” *ACS Appl. Mater. Interfaces*, 2016, 8, 12165–12175.
 20. Jahanshahi, M., Jabari, R., Rashidi, A. M. and Ghoreyshi, A., “Synthesis and Characterization of Thermally-Reduced Graphene,” *Iran. J. Energy Environ.*, 2013, 4, 53–59.
 21. Conway, B. E., “Transition from ‘Supercapacitor’ to ‘Battery’ Behavior in Electrochemical Energy Storage,” *J. Electrochem. Soc.*, 1991, 138, 1539.
 22. P.S. J. and Sutrave, D. S., “A Brief Study of Cyclic Voltammetry and Electrochemical Analysis,” *Int. J. ChemTech Res.*, 2018, 11, 77–88.
 23. Ramadoss A. and Kim, S. J., “Improved activity of a graphene-TiO₂ hybrid electrode in an electrochemical supercapacitor,” *Carbon N. Y.*, 2013, 63, 434–445.
 24. Dreyer, D. R., Murali, S., Zhu, Y., Ruoff, R. S. and Bielawski, C. W., “Reduction of graphite oxide using alcohols,” *J. Mater. Chem.*, 2011, 21, 3443–3447.